



## 3D Modelling of Train Induced Moving Loads on an Embankment

M.Sc. Mojtaba Shahraki, Bauhaus-Universität Weimar, mojtaba.shahraki@uni-weimar.de - M.Sc. M.Sc. Mohamad Reza Salehi Sadaghiani, Bauhaus-Universität Weimar, mohamad.salehi@uni-weimar.de - Prof. Dr.-Ing Karl Josef Witt, Bauhaus-Universität Weimar, kj.witt@uni-weimar.de - Dr.-Ing Thomas Meier, Baugrund Dresden Ingenieurgesellschaft mbH, meier@baugrund-dresden.de

Increasing traffic intensity and train speed in modern railway tracks require complex analysis with focus on dynamic soil behavior. Proper modelling of the dynamic behavior of the railway track system (railway track, trainload, embankment materials and subsoil) is essential to obtain realistic results. This paper presents preliminary results of numerical modelling in PLAXIS 3D for simulating moving loads on a typical soil embankment, which is designed for high-speed railway trains. For this purpose, several static point loads were applied along the railway track. The amount of load is equal to the axle load of the train. For each point load, a dynamic multiplier is assigned as a time-shear force signal. A beam under unit loads on the elastic foundation was modeled for calculation of shear forces. The resulting shear forces in the beam were applied to the 3D model as factors of the dynamic multiplier. In addition, different constitutive soil models such as Linear Elastic (LE), Mohr-Coulomb (MC) and Hardening Soil small-strain (HS-small) were used to approximate the dynamic behavior of the soil embankment.

➤ In terms of structural dynamics, a moving load changes its place during the time and compared to a static load, it can significantly increase displacements in the structure. Moreover, it causes different soil behavior, which has not been fully investigated so far. The dynamic deformation that is caused by trains is normally inelastic. The cumulative plastic deformations during track's lifetime increase progressively and its amount depends on several factors, among them on the subsoil parameters. Irregularities in the track level are common phenomena due to the spatial variation of subsoil and, to some extent the embankment. This degradation of the track is known as differential track settlement [1].

High train speeds demand smaller differential settlement, which must be considered in the modelling of the rail-embankment-subsoil-system by reducing the model error. Another important problem to address is that, after a critical speed, great dynamic amplification appears in the dynamic response of the system, which shows again the importance of the modelling to detect this critical speed of the rail-embankment-subsoil-system [2]. Due to the importance of the moving and dynamic loads, several studies deal with this problem, especially for high-speed railway trains [3, 4].

In case of the numerical simulation, Vogel et al. (2011) carried out a study about dynamic stability of railway tracks on soft soils. They have modeled a train railway embankment in PLAXIS 2D and the numerical results have been compared to experimental data [5]. Correia et al. (2007) also accomplished a preliminary study of comparative suitability of 2D modelling with different numerical tools such as PLAXIS 2D and other finite element software [6]. In recent studies, the effect of the third dimension is considered by some assumptions, for example, Yang and Hung (2001) suggested a so called 2.5 D model for moving loads [7].

The reliability of the models depends largely on the accuracy of the model, the input data and the choice of an appropriate underlying theory. In this respect, the presented results are based on 3D modelling and a first contribution to provide a method for modelling of moving loads.

### Simulation Approach

The moving-loads-induced reactions at the track differ significantly depending on trainloads and speed. When the loads travel on a beam, they do not affect only under the impact points; these loads have also effect on the adjacent parts (away from the impact points of the loads) of the beam.

To consider the effect of the moving loads, the authors have statically analyzed the beam to approximate the length of the shear force distribution in the rail and then those distances are taken into account to extend the length of the model. To estimate shear forces in the rail, a static analysis based on the theory of 'beam on the elastic foundation' has been computed by using PROKON (Structural Analysis and Design software). PROKON performs a linear analysis in which the beam is modeled as a 2D frame on a series of springs with very short distances [8]. The shear forces that were obtained from this analysis have been used as the dynamic multipliers for each point load in PLAXIS 3D.

It has been assumed that the distance between two supports are too small and contacted support along the beam has been provided by the underlying soil. Furthermore, the beam is significantly thin; hence, the external loads are transferred to the support directly (See Figure 1).

The length of the train axles ' $L$ ' controls the length of the model. Moreover, this length has been extended ' $0.18L$ ' on both sides of the beam for considering the effect of the shear force on the adjacent parts of the impact points of the loads.



It has been supposed that the dynamic loads have effect over a greater length of the beam than static loads, and the effect of each axle is felt further away, hence, another length of '0.12L' is added to each side of the beam, to consider the dynamic impact of the loads. Therefore, the optimal length of model could be suggested as ' $L_m = L + 2(0.12 + 0.18)L$ ' (see Table 1).

To approximate the shear forces in a standard railway track, a beam with length ' $L_m$ ' and pin supports in every 60 cm ( $a = 60$ ) laying on soil was considered. A dynamic multiplier is defined as a time-shear force signal in PLAXIS 3D. In the model, every single dynamic point load has its own multiplier. In other words, the dynamic point load is multiplied with the value of signal in every time step. These load multipliers represent the shear forces in the beam due to the static load along the rail in the specific time. The time interval of the multiplier signal has to be considered sufficiently small to prevent miscalculation in FE simulations. The time step is constant because the train speed and the distance between dynamic point loads are constant. For example, a train with speed 180 km/h passes every 30 cm in 0.006 sec, hence, the time interval must be chosen 0.006 sec for the fixed dynamic point loads [9].

The dynamic point loads are located in distances of ' $a/2$ ', to consider the maximum shear forces in the middle of the spans. The distance between the dynamic point loads can be reduced to minimize the model error; but it increases the calculation time. A total number of ' $4(L_m/a)$ ' dynamic point loads for two rails are defined (Figure 2 & Table 1).

### Example

In Figure 2 and Table 1 the relevant information for the model can be found. In the example simulation, the train speed is 180 km/h, and the distance between each dynamic point load is 30 cm. The train passes every 30 cm in 0.006 sec (time step). Consequently, the first axle of the train needs 0.702 sec to pass all 117 dynamic point loads.

Distance between the first and the last wagon axles [m]	$L$	21.7
Additional length for model [m]	$L_a = 0.3L$	6.5
Total additional length (right and left) [m]	$L_{a,total} = 2 \cdot 0.3L$	13.0
Model length [m]	$L_m = L + 0.6L$	34.7
Sleepers distance [m]	$a$	0.6
Dynamic loads distance [m]	$a/2$	0.3
Number of dynamic loads for one rail [-]	$(2L_m)/a$	117
Number of dynamic loads for whole model (two rails) [-]	$(4L_m)/a$	234

Table 1: Model parameters for modelling the moving loads

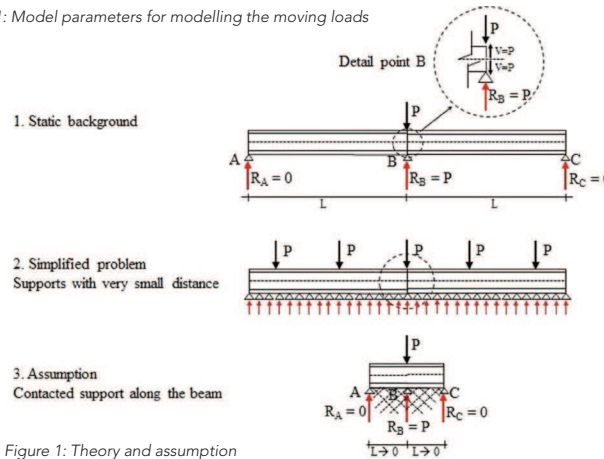


Figure 1: Theory and assumption

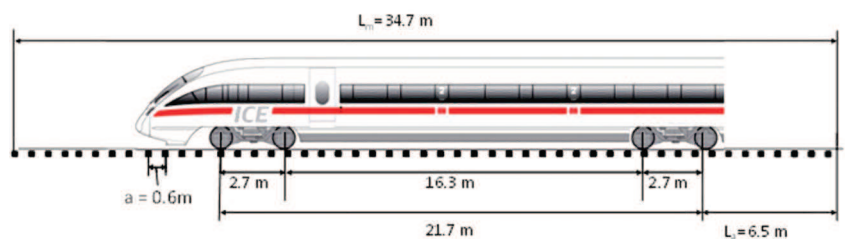


Figure 2: Dimensions of an ICE train and calculated lengths for model

For each time step all of the point loads acquire their values based on the PROKON outputs. In this way, the point loads will be activated continuously and they reach the maximum values when the train axles pass over them (See Table 2).

The distance between the first and the last axle for an ICE is 21.7 m, which in terms of time is 0.434 sec for a train with speed of 180 km/h. The total time that the last axle of the train needs to pass the length of the model is 1.136 sec. In this time, the effect of the train before entering and after leaving the model was also considered.

An additional time of 0.112 sec, which denotes eighteen added rows to the multiplier was considered for relaxing and preventing of miscalculations in the model to the effect of stress wave reflection in dynamic calculations. Various methods are used for modelling boundaries that decrease the effect of wave reflection. Nine multiplier rows with values (shear forces) equal to zero are inserted in the beginning and the end of the multiplier. A small part of the multipliers' sequence is shown in Table 2 and schematic view of multipliers change during the time is illustrated in Figure 3.

The static analysis for the calculation of shear forces was performed by applying four unit point

value used for K. Figure 5 illustrates the calculated shear force in the beam. The length of the model in PROKON was rescaled to the model length used in the PLAXIS model.

**Geometry of 3D-model**

The length of the model for X and Y direction is 35 meters. Due to the geological conditions a model with the depth of 11 m has been considered. Standard fixities and absorbent boundaries were applied in the model to reduce wave reflection at the boundaries. A typical railway track includes rails, rail clips (rail fastening system), and sleepers while all these track elements rest on ballast and subsoil with different soil layers.

The rail is modeled with a beam element along 35 m of profile in Y direction with rectangular cross section. The properties of the beam section are considered in such a way that it has the same properties as a rail (UIC 60). The rail clips are modeled as node to node anchor elements. Each of the sleepers is connected to the rail with two rail clips with 30 cm thickness. The standard sleeper B70 is modeled as a beam element by providing the moment of inertia and area. 68 sleepers are placed in the model with a center-to-center distance of 60 cm. Figure 6 shows the model in PLAXIS 3D. Active dynamic point loads are defined

HS-small model, besides the basic parameters, oedometric, tangent, un/reloading Young's modulus, reference shear modulus and shear strain as well as the advanced parameters are calculated from the secant modulus [11].

Small values of cohesion in shallow depth for simulation with the HS-small constitutive model, particularly for gravel materials leads to unreliable outcomes [12], hence, greater values of cohesion are chosen for the upper soil layers.

Moreover, the first layer (Ballast) is modeled with MC rather than HS-small constitutive model; because of small vertical stresses in the upper layers, the hardening soil constitutive model tend to deliver unrealistic results. Soil basic and advanced properties in models are listed in Table 3 and Table 4. The applied poisson's ratio for all layers in the HS-small model is the default value of PLAXIS ( $\nu_{ur} = 0.2$ ).

To define a node to node anchor in PLAXIS, the maximum forces that the element can carry in tension as well as compression are demanded. In addition, it needs only one stiffness parameter, which is the axial stiffness [13]. The properties of rail clips and the needed parameters for modelling of beam element are listed in Table 5 and Table 6.

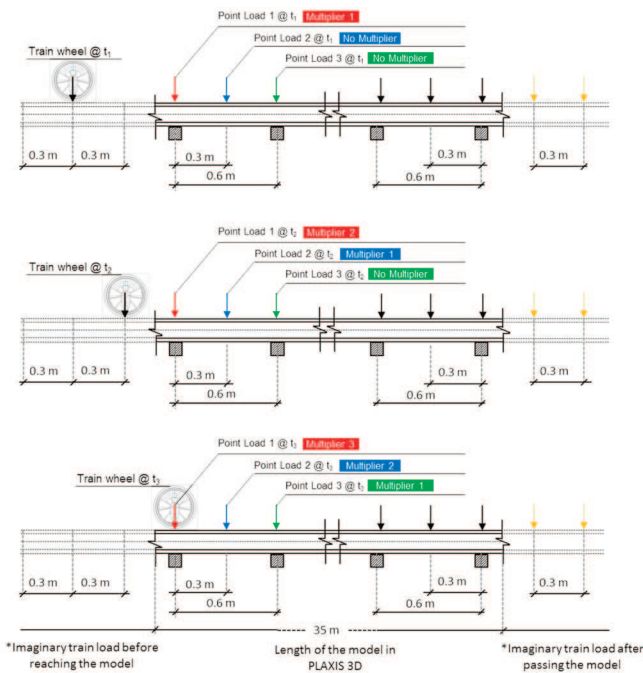


Figure 3: Pictorial representation of multipliers sequence for 117 point loads in the PLAXIS model

loads on the beam to simulate four axle's forces of one wagon. The beam with pin supports every 60 cm are placed on soil. Figure 4 shows the position of four unit point loads, rail and sleepers in PROKON. For this calculation, the default parameters of PROKON (see Figure 4) were used. The modulus of subgrade reaction, K, is a conceptual relationship between the soil pressure and deflection of the beam. Because the beam stiffness is usually ten or more times as large as the soil stiffness as defined by K, the bending moments in the beam and calculated soil pressures are normally not very sensitive to the

loads on track 1 (Figure 6-b). For better visualization of the 3D model, the modeled point loads are deactivated in Figure 6-a and 6-b. Figure 6-c shows exemplary some dynamic point loads.

**Material Properties**

Saturated, unsaturated density, Poisson's ratio and shear modulus were available from geotechnical investigations, which were used for modelling of soil behavior with the linear elastic constitutive model. Secant modulus, friction angle, cohesion and dilatancy of materials were acquired from literature [10]. To model the soil behavior with the

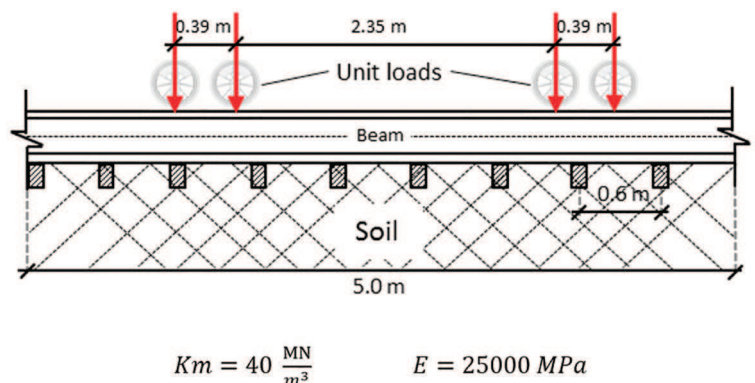


Figure 4: Scaled static model of unit loads of the beam in PROKON

**Calculation Phases and Results**

The calculation consists of three phases. The first phase is common for generating the initial stresses with active groundwater table. A plastic drained calculation type is chosen in phase two. In this phase, all elements of the railway track (sleepers, rails and rail clips) should be active. The dynamic option should be selected in phase three to consider stress waves and vibrations in the soil. In this phase, all dynamic point loads on the rails are active.

The simulations (SIM1 and SIM2) are performed for a train (one wagon) speed of 180 km/h with

117 Multipliers

Time steps	Distance [m]	Time [s]	Multiplier					
			1	2	3	116	117	
1	0	0	0	0	0	...	0	0
...	...	...	...	...	...	...	...	...
7	0	0	0	0	0	...	0	0
8	0.3	0.006	0	0	0	...	0	0
9	0.6	0.012	-0.001	0	0	...	0	0
10	0.9	0.018	-0.0012	-0.001	0	...	0	0
...	...	...	...	...	...	...	...	...
229	66.3	1.326	0	0	0	...	0.0001	-0.0005
230	66.6	1.332	0	0	0	...	0	0.0001

Table 2: Sequence of multipliers for all point loads

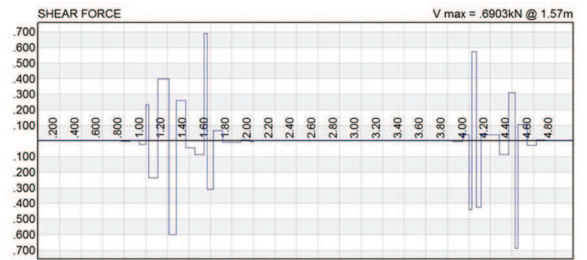


Figure 5: Shear force in the beam

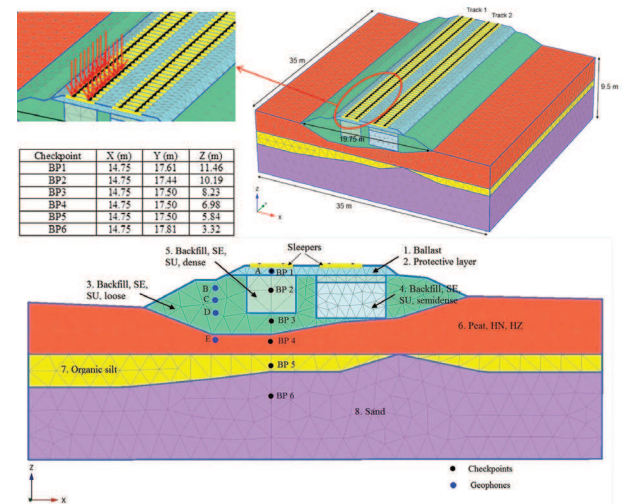


Figure 6: Details of the model

No.	Soil layers	$\gamma_{sat}$	$\gamma_{unsat}$	$\nu$	$\phi'$	$c'$	$\Psi$	$E'$
		[kN/m <sup>3</sup> ]	[kN/m <sup>3</sup> ]	[-]	[°]	[kN/m <sup>2</sup> ]	[°]	[kN/m <sup>2</sup> ]
1	Ballast	21	19	0.30	35	30	5	30000
2	Protective layer	23	22	0.25	40	30	15	55000
3	Backfill, SE, SU, loose	19	18	0.35	28	10	0	25000
4	Backfill, SE, SU, semidense	20	19	0.35	28	10	0	35000
5	Backfill, SE, SU, dense	20	19.5	0.35	28	10	0	43000
6	Peat, HN, HZ	11	11	0.35	26	15	0	2000
7	Organic silt	13	13	0.35	25	10	0	4000
8	Sand	20	19	0.35	40	5	10	80000

Table 3: Basic material properties of the soil layers for LE and MC models

No.	Soil layers	$m$	$E_{oed}^{ref}$	$E_{co}^{ref}$	$E_{ur}^{ref}$	$E_{30}$	$G_{30} = G_o^{ref}$	$\gamma_{0.7}$
		[-]	[kN/m <sup>2</sup> ]	[-]				
6	Peat, HN, HZ	0.7	2000	2000	6000	8100	3000	$6.29 \times 10^{-3}$
7	Organic silt	0.7	4000	4000	12000	16200	6000	$2.79 \times 10^{-3}$
8	Sand	0.5	80000	80000	240000	270000	100000	$1.81 \times 10^{-4}$

Table 4: Advanced material properties of the soil layers for HS-small model

Parameter	Unit	Rail	Sleeper
Cross section area (A)	[m <sup>2</sup> ]	$7.7 \times 10^{-3}$	$5.13 \times 10^{-2}$
Unit weight ( $\gamma$ )	[kN/m <sup>3</sup> ]	78	25
Young's modulus (E)	[kN/m <sup>2</sup> ]	$200 \times 10^6$	$36 \times 10^6$
Moment of inertia around the second axis (I <sub>2</sub> )	[m <sup>4</sup> ]	$3.055 \times 10^{-5}$	0.0253
Moment of inertia around the third axis (I <sub>3</sub> )	[m <sup>4</sup> ]	$5.13 \times 10^{-6}$	$2.45 \times 10^{-4}$

Table 5: Input properties in PLAXIS 3D for rail and sleeper

Maximum tension force $ F_{max,ten} $	312 kN
Maximum compression force $ F_{max,com} $	1716 kN
Axial stiffness (EA)	$2 \times 10^6$ kN

Table 6: Rail clip's properties

consideration of three different constitutive soil models. In SIM1, for all soil layers the Linear Elastic (LE) model was used. SIM2 was simulated using a combination of Mohr-Coulomb (MC) and Hardening Soil small-strain model (HS-small). Here, upper soil layers are modeled with the MC model and the deepest three soil layers are modeled with the HS-small model [12].

In dynamics, velocities rather than displacements are presented to avoid second integration leading to increasing errors in low frequency domain [14]. The velocity amplitude decreases by propagation of the wave to the deeper soil layers. Material and geometric damping are the main reasons for the decreasing velocity amplitude in deep layers. In this model, both types of damping are considered by applying Rayleigh damping coefficients. The lowest and highest relevant frequencies

Constitutive model	Wagons No.	Train speed 180 km/h					
		Vertical velocity (mm/s) in different checkpoints					
		BP1	BP2	BP3	BP4	BP5	BP6
SIM 1	1	27.15	4.54	1.38	0.74	0.23	1.2
SIM 2	1	28.90	9.40	2.51	1.40	0.58	0.16

Table 7: Estimated velocities for train with speed of 180 km/h

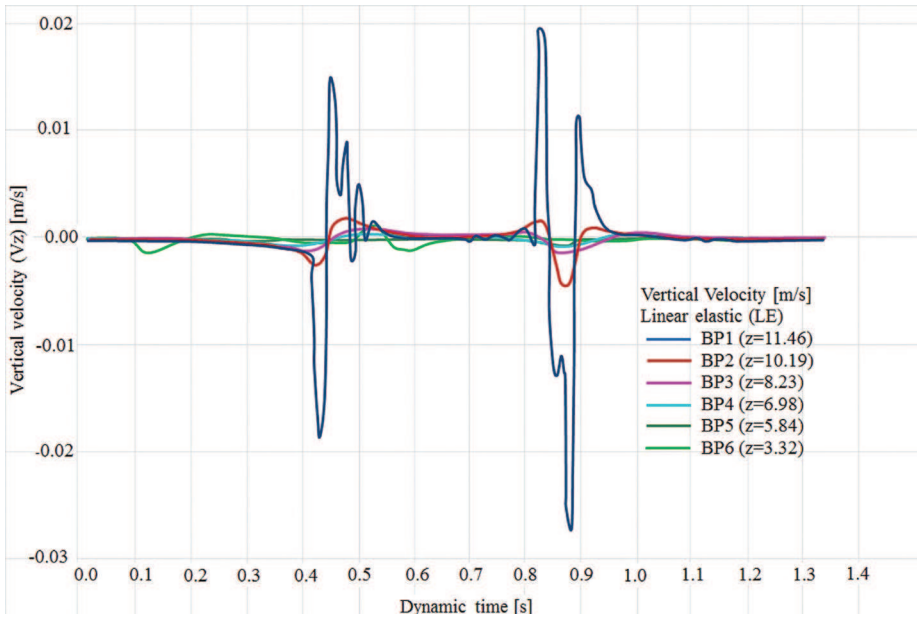


Figure 7: Vertical velocity, LE-Model, 180 Km/h

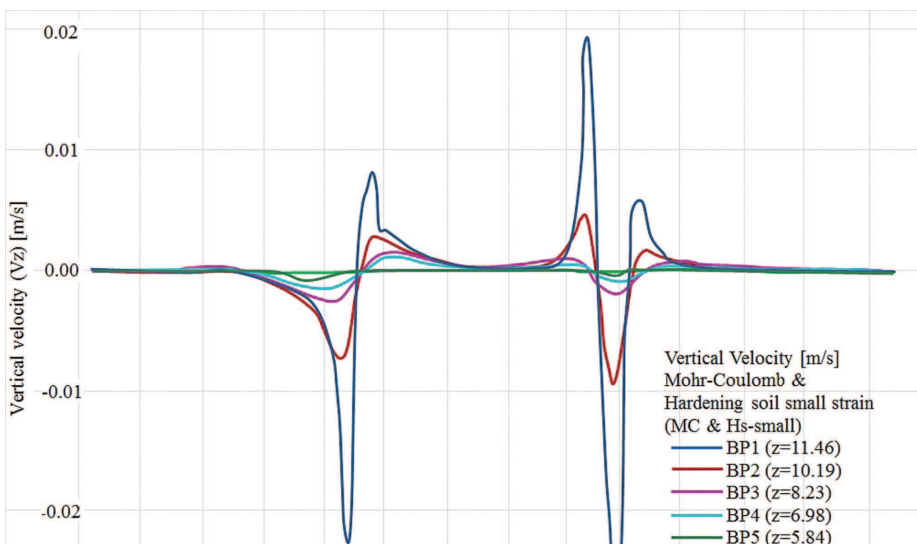


Figure 8: Vertical velocity, HS-small & MC-Model, 180Km/h

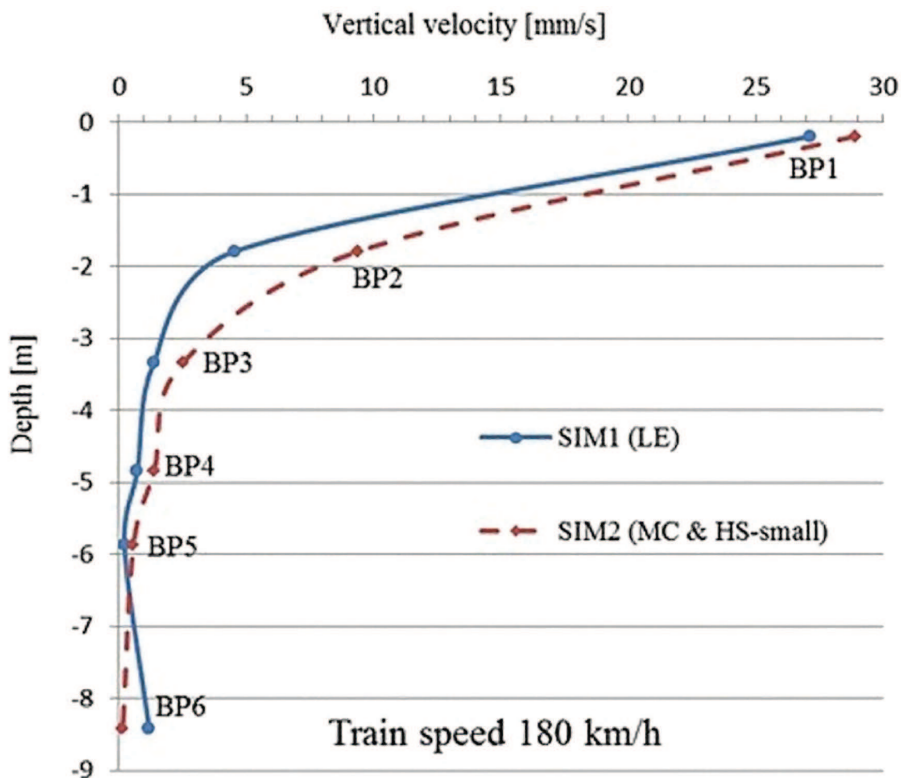


Figure 9: Estimated velocities for train with speed of 180 km/h in checkpoints

depend upon the model properties and train speed. In this study, the lowest and highest frequencies for estimation of the Rayleigh damping coefficients are assumed to be between 10 and 100 Hertz.

Table 7 summarizes the results of the simulations in terms of velocity (mm/s) for four checkpoints in different soil layers. Moreover, velocity amplitudes are decreased by going to the depth, which is matched to the engineering expectation. The checkpoints BP5 and BP6 show smaller velocities as the wave goes deeper in Z-direction. Velocity changes in each checkpoint by passing the train for both models are shown in Figure 7 and 8. Figure 9 shows a comparison between the calculated maximum velocities in checkpoints of two simulations (SIM1 and SIM2). The highest velocity belongs to the checkpoint BP1 that is located in shallowest depth under the railway. SIM2 estimated smaller values for deeper checkpoints than SIM1, while in shallow depth, it points out higher velocity compared to the SIM1. However, both simulations show a similar trend in the results.

#### Conclusion

Moving loads can be modeled in PLAXIS 3D by applying the proposed approach and the help of auxiliary software. This proposed approach has also a big limitation. For defining the moving loads, all multipliers have to be assigned manually to each dynamic point load. For getting more accurate results, one could divide the distance between the sleepers in four or even eight parts. By adding more point loads, it is possible to get more detailed results. With this method, one could also model the break effect as

well as the interaction of two trains, which are moving in opposite directions. This approach provides a way for investigating moving loads in PLAXIS. Real 3D modelling of moving loads in PLAXIS 3D was done here successfully. These models have to be evaluated through comparison with results from experiments and theoretical analysis. The validation of these models will be accomplished in next phase of this project. Geotechnical applications require advanced constitutive models for the simulation of the non-linear and time-dependent behavior of soils. Although the modelling of the soil itself is an important issue, many geotechnical engineering projects involve the modelling of complex geotechnical problems such as the moving loads. Therefore, future versions of the PLAXIS software will be equipped with special features to deal with the moving loads.

#### References

- T. Dahlberg, "Railway track settlements - a literature review," Linköping, Sweden 2004.
- C. Madshus and A. M. Kaynia, "High-Speed Railway Lines on Soft Ground: Dynamic Behaviour at Critical Train Speed," Journal of Sound and Vibration, vol. 231, pp. 689-701, 2000.
- L. Hall, "Simulations and analyses of train-induced ground vibrations in finite element models," Soil Dynamics and Earthquake Engineering, 2003.
- S. Witt, "The Influence of Under Sleeper Pads on Railway Track Dynamics," Department of Management and Engineering, Linköping University, Sweden, 2008.
- W. Vogel, K. Lieberenz, T. Neidhart, and D. Wegener, "Zur dynamischen Stabilität von Eisenbahnstrecken mit Schotteroberbau auf Weichschichten," 2011.
- B. Coelho, J. Priest, P. Holscher, and W. Powrie, "Monitoring of transition zones in railways," presented at the Railway Engineering Conference England, 2009.
- Y.-B. Yang and H.-H. Hung, "A 2.5D finite/infinite element approach for modelling visco-elastic bodies subjected to moving loads," International Journal for Numerical Methods in Engineering, vol. 51, pp. 1317-1336, 2001.
- Prokon Software Consultants, PROKON User's Guide: Prokon Software Consultants (Pty) Ltd., 2010.
- M. Shahraki, "Numerical Validation of Dynamic Stability Experiments for High-Speed Railway Tracks," Master of Science, Faculty of Civil Engineering - Department of Geotechnical Engineering, Bauhaus-Universität Weimar, Weimar, Germany, 2013.
- D. Rütty and K. J. Witt, Wissensspeicher Geotechnik, 18 ed. Weimar, Germany: Bauhaus-Universität Weimar, 2011.
- Plaxis bv, PLAXIS 3D 2011-Reference vol. 2. Netherlands: PLAXIS, 2011.
- P.-A. v. Wolffersdorff, "Ausgewählte Probleme zu statischen und dynamischen Standsicherheitsberechnungen von Staudämmen," 2010.
- Plaxis bv, PLAXIS 3D 2011-Material-Models vol. 3. Netherlands: PLAXIS, 2011.
- A. G. Correia, J. Cunha, J. Marcelino, L. Caldeira, J. Varandas, Z. Dimitrovová, A. Antão, and M. G. d. Silva, "Dynamic analysis of rail track for high speed trains. 2D approach," in 5th Intl Workshop on Application of Computational Mechanics on Geotechnical Engineering, Portugal 2007, p. 14.